

Application of A Priori Error Estimates for Navier-Stokes Equations to Accurate Finite Element Solution

P. BURDA^{a,1}, J. NOVOTNÝ^{b,1}, J. ŠÍSTEK^{a,1}

^aDepartment of Mathematics
Czech University of Technology
Karlovo náměstí 13, CZ-121 35 Praha 2
CZECH REPUBLIC

^bInstitute of Thermomechanics
Czech Academy of Science
Dolejšková 5, CZ-182 00 Praha 8
CZECH REPUBLIC

Abstract: - In the applications of the finite element method, problems with corner-like singularities (e.g. on the well-known L-shaped domain) are most often solved by the adaptive strategy: the mesh near the corners is refined according to the *a posteriori* error estimates. In this paper we present an alternative approach. For flow problems on domains with corner singularities we use the *a priori* error estimates and asymptotic expansion of the solution to derive an algorithm for refining the mesh near the corner. It gives very precise solution in a cheap way. We present some numerical results.

Key words: - FEM; singularity; refinement; a priori error estimates

1991 MSC: 65M60, 65N30, 76D05

1 Introduction

In the paper we present the application of a priori error estimates of the finite element method (FEM) to solve problems in computational fluid dynamics. We generate the computational mesh in the purpose of uniform distribution of error on elements, and use it in order to get precise solution on domains with corner-like singularities. We apply this approach to incompressible viscous flow modelled by the steady Navier-Stokes equations.

Usual way to improve accuracy of solution by the FEM is the refinement of the mesh near places, where singularity can appear. Another way is the adaptive refinement based on a posteriori error estimates or error estimators. This method could be quite time demanding, since it needs several runs of solution. Completely different method is applied in this paper. Computational mesh is prepared before the first run of the solution.

2 Model problem

We consider two-dimensional flow of a viscous, incompressible fluid modelled by the Navier-Stokes equations in a domain with corner sin-

¹ This research has been supported by the GAAV grant no. IAA2120201/02 and by the State Research Project No. MSM 684 0770010

gularity, see Fig. 1.

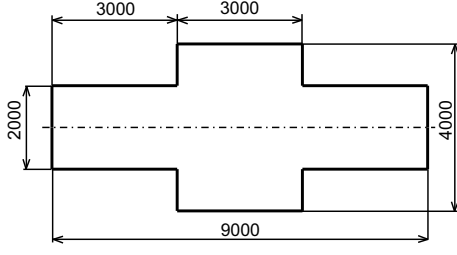


Fig. 1. The geometry of the channel

Due to symmetry, we solve the problem only on the upper half of the channel. Let us denote this domain Ω . The steady Navier-Stokes problem consists in finding the velocity $\mathbf{v} = (v_1, v_2)$, and pressure p defined in Ω and satisfying

$$(\mathbf{v} \cdot \nabla) \mathbf{v} - \nu \Delta \mathbf{v} + \nabla p = \mathbf{0}, \quad (1)$$

$$\nabla \cdot \mathbf{v} = 0 \quad (2)$$

together with boundary conditions on disjoint parts of the boundary Γ_{in} , Γ_{wall} and Γ_{out} (meaning, in turn, the inlet, the wall, and the outlet part)

$$\mathbf{v} = \mathbf{g} \text{ on } \Gamma_{in} \cup \Gamma_{wall} \quad (3)$$

$$\nu \frac{\partial \mathbf{v}}{\partial \mathbf{n}} - p \mathbf{n} = \mathbf{0} \text{ on } \Gamma_{out} \quad ('do \text{ nothing}')$$

We consider kinematic viscosity $\nu = 0.000025$ m²/s and $v_{in \max} = 1$ m/s, which give a maximum Reynolds number around 760.

3 Algorithm for generation of computational mesh

To derive the algorithm, two main 'tools' are used. The first is a priori estimate of the FEM error for the Navier-Stokes equations (1)-(3) (cf. [6])

$$\begin{aligned} \|\nabla(\mathbf{u} - \mathbf{u}_h)\|_{L_2(\Omega)} + \|p - p_h\|_{L_2(\Omega)} &\leq \\ &\leq C \left[\left(\sum_K h_K^{2k} |\mathbf{u}|_{H^{k+1}(T_K)}^2 \right)^{1/2} + \right. \\ &\quad \left. + \left(\sum_K h_K^{2k} |p|_{H^k(T_K)}^2 \right)^{1/2} \right] \end{aligned} \quad (5)$$

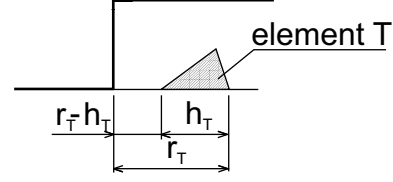


Fig. 2. Description of element variables

where h_K is the diameter of triangle T_K of a triangulation \mathcal{T} , and $k = 2$ for Hood-Taylor elements, which are applied in our calculations.

The second tool is the asymptotic behaviour of the solution near the singularity. In [1], it was proved for the Stokes flow in axisymmetric tubes, that for internal angle $\alpha = \frac{3}{2}\pi$, the leading term of expansion of the solution for each velocity component is

$$u_i(\rho, \vartheta) = \rho^{0.5445} \varphi_i(\vartheta) + \dots, \quad i = 1, 2 \quad (6)$$

where ρ is the distance from the corner, ϑ the angle and φ_i is a smooth function. The same expansion is known to apply to the plane flow (cf. [8]), and similar results were also proved for the Navier-Stokes equations.

Taking into account the expansion (6), we can estimate

$$\begin{aligned} |\mathbf{u}|_{H^{k+1}(T_K)}^2 &\approx C \int_{r_K - h_K}^{r_K} \rho^{2(\gamma - k - 1)} \rho \, d\rho = \\ &= C \left[-r_K^{2(\gamma - k)} + (r_K - h_K)^{2(\gamma - k)} \right] \end{aligned} \quad (7)$$

where r_K is the distance of element T_K from the corner, see Fig. 2.

Putting estimate (7) into the a priori error estimate (5) we derive that we should guarantee

$$h_K^{2k} \left[-r_K^{2(\gamma - k)} + (r_K - h_K)^{2(\gamma - k)} \right] \approx h_{ref}^{2k} \quad (8)$$

in order to get the error estimate of order $O(h_{ref}^k)$ uniformly distributed on elements. From this expression, we compute element diameters in accordance to chosen h_{ref} . Let us note that similar idea was presented by C. Johnson for an elliptic problem in [7].

i	r_i (m)	h_i (m)
1	0.30000	0.06956
2	0.23044	0.05621
3	0.17423	0.04483
4	0.12940	0.03522
5	0.09419	0.02720
6	0.06699	0.02059
7	0.04640	0.01524
8	0.03116	0.01098
9	0.02017	0.00767
10	0.01250	0.00515
11	0.00735	0.00330
12	0.00405	0.00199
13	0.00206	0.00112
14	0.00094	0.00057
15	0.00038	0.00038

Table 1: Resulting refinement

4 Geometry and design of the mesh

The algorithm was applied here to a computational domain in 2D which represents the channel with abruptly extended diameter (Fig. 1). Since this is symmetric, the problem was solved only on the upper half of the channel.

For this channel, we used $h_{ref} = 0.1732$ m, $k = 2$, $\gamma = 0.5444837$ and started in the distance $r_1 = 300$ mm from the corner. This corresponds to cca 3% of relative error on elements. Fifteen diameters of elements were obtained (Table 1).

Note, that those are ‘1D’ data. An experiment with three meshes with different refined details (Fig. 3) was performed (cf. [4],[5], [9] for details). Type C of refinement in Fig. 3 provided the best uniformity of the error on elements, therefore was chosen for further applications. This type of refinement corresponds to the polar coordinate system used in the derivation of the algorithm, and is applied in the experiment described in this paper.

The refined detail is connected to the rest of the coarse mesh. In Fig. 4, final mesh after the refinement is shown.

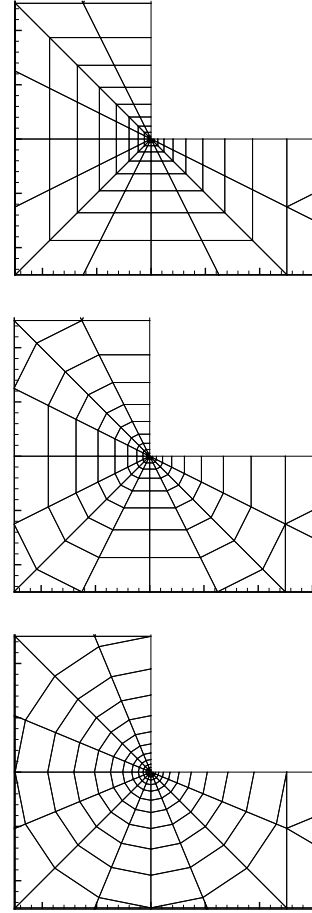


Fig. 3. Details of refined mesh - type A (up), type B (middle), type C (down)

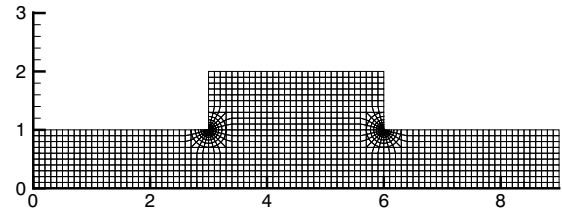


Fig. 4. Final computational mesh for the channel

5 Measuring of error

To review the efficiency of the algorithm, we use a posteriori error estimates to evaluate the obtained error on elements. Suppose now, that the exact solution of the problem is denoted as (u_1, u_2, p) and the approximate solution obtained by the FEM as (u_{1h}, u_{2h}, p_h) . The exact

solution differs from the approximate solution in the error $(e_{u_1}, e_{u_2}, e_p) = (u_1 - u_{1h}, u_2 - u_{2h}, p - p_h)$. For the solution (u_1, u_2, p) we denote

$$\begin{aligned} \mathcal{U}^2(u_1, u_2, p) &= \\ &= \|(u_1, u_2)\|_{H^1(T_K)}^2 + \|p\|_{L_2(T_K)}^2 = \\ &= \int_{T_K} \left(u_1^2 + u_2^2 + \left(\frac{\partial u_1}{\partial x_1} \right)^2 + \left(\frac{\partial u_1}{\partial x_2} \right)^2 + \right. \\ &\quad \left. + \left(\frac{\partial u_2}{\partial x_1} \right)^2 + \left(\frac{\partial u_2}{\partial x_2} \right)^2 \right) d\Omega + \int_{T_K} p^2 d\Omega \end{aligned}$$

The following estimate of error is used (see e.g. [2])

$$\mathcal{U}^2(u_1 - u_{1h}, u_2 - u_{2h}, p - p_h) \leq \quad (9)$$

$$\leq \mathcal{E}^2(u_{1h}, u_{2h}, p_h) \quad (10)$$

where

$$\begin{aligned} \mathcal{U}^2(u_1 - u_{1h}, u_2 - u_{2h}, p - p_h) &= \\ &= \|(e_{u_1}, e_{u_2})\|_{H^1(T_K)}^2 + \|e_p\|_{L_2(T_K)}^2, \\ \mathcal{E}^2(u_{1h}, u_{2h}, p_h) &= C \left[h_K^2 \int_{T_K} (\mathfrak{R}_1^2(u_{1h}, u_{2h}, p_h) + \right. \\ &\quad \left. + \mathfrak{R}_2^2(u_{1h}, u_{2h}, p_h)) d\Omega + \int_{T_K} \mathfrak{R}_3^2(u_{1h}, u_{2h}, p_h) d\Omega \right] \end{aligned}$$

where \mathfrak{R}_1 , \mathfrak{R}_2 , and \mathfrak{R}_3 stand for the residuals, see [3]. The constant C is determined from a numerical experiment (cf. [3]).

Usual way to ‘measure’ the error on elements is to compute the error related to the computed solution, i.e. relative error. This is given by the ratio of absolute norm of the solution error related to unit area of element T_K

$$\frac{1}{|T_K|} \mathcal{E}^2(u_{1h}, u_{2h}, p_h, T_K)$$

to the solution norm on the whole domain Ω related to unit area of Ω

$$\frac{1}{|\Omega|} \mathcal{U}^2(u_{1h}, u_{2h}, p_h, \Omega)$$

i.e.

$$\begin{aligned} \mathcal{R}^2(u_{1h}, u_{2h}, p_h, T_K) &= \\ &= \frac{|\Omega| \mathcal{E}^2(u_{1h}, u_{2h}, p_h, T_K)}{|T_K| \mathcal{U}^2(u_{1h}, u_{2h}, p_h, \Omega)} \end{aligned} \quad (11)$$

But for the similarity with a priori error estimate, we use the modified absolute error defined as

$$\begin{aligned} \mathcal{A}_m^2(u_{1h}, u_{2h}, p_h, T_K, \Omega, n) &= \\ &= \frac{|\Omega| \mathcal{E}^2(u_{1h}, u_{2h}, p_h, T_K)}{|\overline{T_K}| \mathcal{U}^2(u_{1h}, u_{2h}, p_h, \Omega)} \end{aligned} \quad (12)$$

where $|\overline{T_K}|$ is the mean area of elements obtained as $|\overline{T_K}| = \frac{|\Omega|}{n}$, and n denotes the number of all elements in the domain.

6 Numerical results

In Figures 5 - 8, plots of entities that characterize the flow in the channel are presented. In Figures 5 and 6, there are streamlines and plot of velocity component u_x . Plots of velocity component u_y and pressure are in Figures 7 and 8. The data correspond to the Reynolds number $Re = 400$.

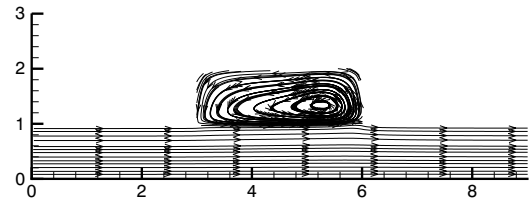


Fig. 5. Streamlines

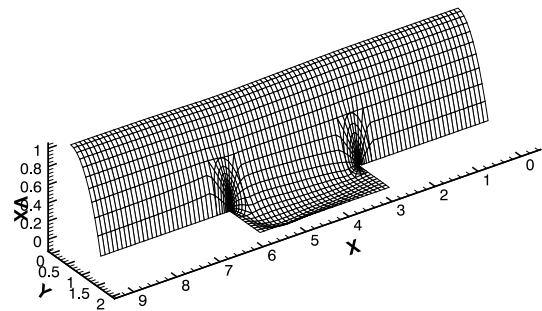


Fig. 6. Velocity component u_x

In Fig. 10, there are values of obtained error on elements in refined area. All obtained values are listed in Table 2. Marking of elements for Table 2 is described in Fig. 9.

	A	B	C	D	E	F	G	H	I	J	K
1	1.276	0.446	0.134	0.049	0.037	0.034	0.040	0.042	0.044	0.044	0.047
2	1.413	0.461	0.083	0.035	0.039	0.044	0.048	0.053	0.058	0.065	0.076
3	1.561	0.411	0.079	0.045	0.048	0.054	0.059	0.065	0.070	0.077	0.088
4	1.610	0.354	0.077	0.051	0.056	0.062	0.067	0.072	0.077	0.082	0.089
5	1.582	0.304	0.076	0.053	0.058	0.063	0.067	0.071	0.076	0.084	0.112
6	1.423	0.251	0.070	0.049	0.054	0.057	0.061	0.065	0.071	0.090	0.131
7	1.115	0.189	0.055	0.039	0.044	0.046	0.042	0.053	0.063	0.087	0.121
8	0.699	0.116	0.037	0.025	0.028	0.030	0.033	0.039	0.053	0.076	0.098
9	0.229	0.044	0.016	0.013	0.015	0.018	0.023	0.032	0.050	0.074	0.099
10	0.262	0.045	0.017	0.019	0.022	0.027	0.033	0.044	0.063	0.091	0.120
11	0.073	0.112	0.036	0.034	0.038	0.038	0.052	0.064	0.084	0.110	0.134
12	1.129	0.186	0.054	0.047	0.052	0.059	0.068	0.082	0.101	0.122	0.135
13	1.434	0.245	0.066	0.055	0.061	0.070	0.080	0.095	0.112	0.127	0.130
14	1.574	0.299	0.072	0.058	0.063	0.074	0.086	0.101	0.117	0.127	0.127
15	1.633	0.350	0.071	0.056	0.061	0.072	0.085	0.101	0.116	0.126	0.131
16	1.511	0.402	0.072	0.051	0.054	0.066	0.079	0.094	0.110	0.123	0.135
17	1.398	0.450	0.073	0.044	0.049	0.059	0.071	0.085	0.099	0.115	0.138
18	1.266	0.441	0.133	0.054	0.049	0.053	0.065	0.074	0.085	0.097	0.124

Table 2: Obtained errors on elements

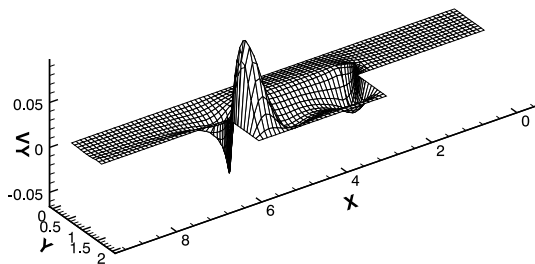


Fig. 7. Velocity component u_y

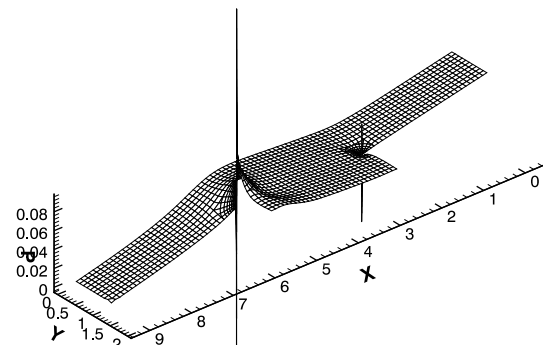


Fig. 8. Pressure

7 Conclusion

Numerical results give satisfactory confirmation of the algorithm. The application of *a priori* error estimates of the finite element method for mesh refinement near the singularity is very efficient for our problem. This can be seen espe-

cially on the errors indicated on elements: the errors are distributed very uniformly.

The algorithm is applied to design the mesh close to an internal angle of $\frac{3}{2}\pi$. Nevertheless it

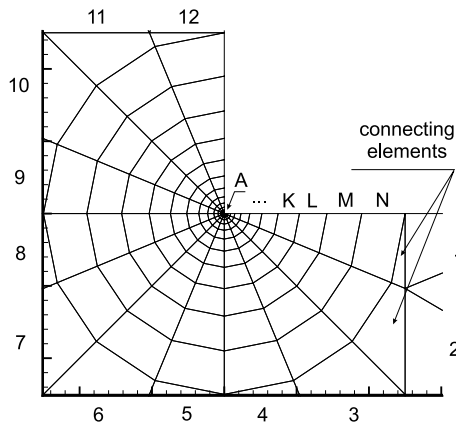


Fig. 9. Marking of elements for Table 2

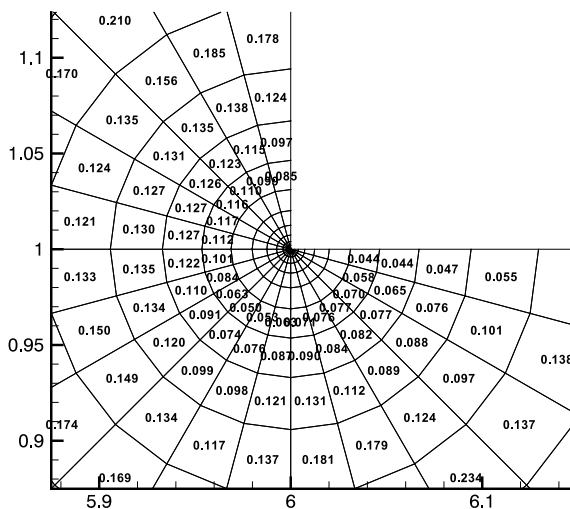


Fig. 10. Errors on elements in the refined area

References

- [1] P. Burda, On the FEM for the Navier-Stokes equations in domains with corner singularities. In: *M. Křížek, et al., editors. Finite Element Methods, Superconvergence, Post-Processing and A Posteriori Estimates*, Marcel Dekker, New York, 1998, 41-52
- [2] P. Burda, A posteriori error estimates for the Stokes flow in 2D and 3D domains. In: *P. Neittaanmäki, M. Křížek, editors. Finite Element Methods, 3D.(GAKUTO Internat. Series, Math. Sci. and Appl., Vol. 15)*, Gakkotosho, Tokyo, 2001, 34-44
- [3] P. Burda, J. Novotný, B. Sousedík, A posteriori error estimates applied to flow in a channel with corners, *Mathematics and Computers in Simulation*, **61** (2003), 375-383
- [4] P. Burda, J. Novotný, B. Sousedík, J. Šístek, Finite Element Mesh Adjusted to Singularities Applied to Axisymmetric and Plane Flow. In: *M. Feistauer, et al., editors. Numerical Mathematics and Advanced Applications, ENUMATH 2003*, Springer, Berlin, 2004, 186-195
- [5] P. Burda, J. Novotný, J. Šístek, Precise FEM solution of corner singularity using adjusted mesh applied to axisymmetric and plane flow, *Int. J. Num. Meth. Fluids*, **47**, 2005, pp. 1285 - 1292.
- [6] V. Girault, P. G. Raviart, *Finite Element Method for Navier-Stokes Equations*, Springer, Berlin, 1986
- [7] C. Johnson, *Numerical Solution of Partial Differential Equations by the Finite Element Method*, Cambridge University Press, 1994
- [8] V. A. Kondratiev, Asimptotika rešenija uravnenija Nav'je-Stoksa v okrestnosti uglovoj točki granicy, *Prikl. Mat. i Mech.*, **1** (1967), 119-123
- [9] J. Šístek, *Stabilization of finite element method for solving incompressible viscous flows*, Diploma Thesis, ČVUT, Praha, 2004.